The Astrophysical Journal, 824:83 (6pp), 2016 June 20 doi:10.3847/0004-637X/824/2/83

REVISITING THE MICROLENSING EVENT OGLE 2012-BLG-0026: A SOLAR MASS STAR WITH TWO COLD GIANT PLANETS

J.-P. Beaulieu[1,2,3], D. P. Bennett[4,5], V. Batista[1], A. Fukui[6], J.-B. Marquette[1], S. Brillant[7], A. A. Cole[3], L. A. Rogers[8,9,16], T. Sumi[10], F. Abe[11], A. Bhattacharya[3,4], N. Koshimoto[10], D. Suzuki[3,4], P. J. Tristram[12], C. Han[13], A. Gould[14], R. Pogge[14], and J. Yee[15,16]

[1] Sorbonne Universités, UPMC Univ Paris 6 et CNRS, UMR 7095, Institut d'Astrophysique de Paris, 98 bis bd Arago, F-75014 Paris, France; beaulieu@iap.fr, batista@iap.fr, marquett@iap.fr
[2] LESIA Observatoire de Paris, Section de Meudon 5, place Jules Janssen F-92195 Meudon, France
[3] School of Physical Sciences, University of Tasmania, Private Bag 37 Hobart, Tasmania 7001 Australia; Andrew.Cole@utas.edu.au
[4] University of Notre Dame, Department of Physics, 225 Nieuwland Science Hall, Notre Dame, IN 46556-5670, USA; bennett@nd.edu, suzuki@nd.edu
[5] Laboratory for Exoplanets and Stellar Astrophysics, NASA/Goddard Space Flight Center, Greenbelt, MD 20815, USA
[6] Okayama Astrophysical Observatory, National Astronomical Observatory of Japan, Asakuchi, Okayama 719-0232, Japan; afukui@oao.nao.ac.jp
[7] European Southern Observatory (ESO), Karl-Schwarzschildst. 2, D-85748 Garching, Germany; sbrillan@eso.org
[8] Department of Astronomy and Astrophysics, 5640 S. Ellis Avenue, Chicago, IL 60637, USA; larogers@uchicago.edu
[9] Department of Earth and Planetary Science, University of California at Berkeley, 501 Campbell Hall 3411, Berkeley CA, 94720, USA
[10] Department of Earth and Space Science, Graduate School of Science, Osaka University, Toyonaka, Osaka 560-0043, Japan; sumi@ess.sci.osaka-u.ac.jp
[11] Institute for Space-Earth Environmental Research, Nagoya University, Nagoya University, Nagoya 464-8601, Japan
[12] Mt. John University Observatory, P.O. Box 56, Lake Tekapo 8770, New Zealand
[13] Department of Physics, Chungbuk National University, Cheogju 361-763, Korea; cheongho@astroph.chungbuk.ac.kr
[14] Department of Astronomy, Ohio State University, 100 W 18th Avenue, Columbus, OH 43210, USA; gould@osu.edu, pogge.1@osu.edu
[15] Harvard-Smithsonian Center for Astrophysics, 60 Garden Street, MS-15, Cambridge, MA 02138, USA; jyee@cfa.harvard.edu
Received 2016 January 8; accepted 2016 March 4; published 2016 June 15

ABSTRACT

Two cold gas giant planets orbiting a G-type main-sequence star in the galactic disk were previously discovered in the high-magnification microlensing event OGLE-2012-BLG-0026. Here, we present revised host star flux measurements and a refined model for the two-planet system using additional light curve data. We performed high angular resolution adaptive optics imaging with the Keck and Subaru telescopes at two epochs while the source star was still amplified. We detected the lens flux, $H = 16.39 \pm 0.08$. The lens, a disk star, is brighter than predicted from the modeling in the original study. We revisited the light curve modeling using additional photometric data from the B&C telescope in New Zealand and CTIO 1.3 m *H*-band light curve. We then include the Keck and Subaru adaptive optic observation constraints. The system is composed of a ~4–9 Gyr lens star of $M_{\rm lens} = 1.06 \pm 0.05\,M_{\odot}$ at a distance of $D_{\rm lens} = 4.0 \pm 0.3$ kpc, orbited by two giant planets of $0.145 \pm 0.008\,M_{\rm Jup}$ and $0.86 \pm 0.06\,M_{\rm Jup}$, with projected separations of 4.0 ± 0.5 au and 4.8 ± 0.7 au, respectively. Because the lens is brighter than the source star by $16 \pm 8\%$ in H, with no other blend within one arcsec, it will be possible to estimate its metallicity using subsequent IR spectroscopy with 8–10 m class telescopes. By adding a constraint on the metallicity it will be possible to refine the age of the system.

Key words: gravitational lensing: micro – planets and satellites: detection – planets and satellites: gaseous planets

1. INTRODUCTION

Over the last 20 years, several methods probing different sections of the exoplanet zoo have been used: radial velocity, stellar transits, direct imaging, pulsar timing, transit timing, astrometry, and gravitational microlensing. These discoveries have already challenged and revolutionized our theories of planet formation and dynamical evolution. Of the nearly 2000 confirmed planets known to date, 488 of them are in multi-planet systems, including two unusual systems with two cold gas giant planets, discovered by microlensing. The first one (OGLE-2006-BLG-109Lb, c) is a half-scale model of our solar system (Gaudi et al. 2008; Bennett et al. 2010). The second one, detected in the microlensing event OGLE-2012-BLG-0026, is composed of two giant planets orbiting a G-type main-sequence star (Han et al. 2013, H2013 hereafter).

H2013 identified four possible sets of system parameters as a consequence of the well-known close/wide degeneracy in the lens equation. They estimated the physical parameters using a parallax constraint and a measurement of the Einstein ring radius. They also noted a significant contribution of blended (unmagnified) flux to the light curve and recognized that sub-arcsecond imaging is required in order to separate the source +lens from possible contamination by unrelated stars. This deblending is critical in order to properly estimate the brightness of the lens; such a measurement can then be used to refine the light curve model and decrease uncertainties on the physical parameters of the system. Here we follow the approach described in detail by Batista et al. (2014, 2015). We measure the lens flux in the microlensing event OGLE-2012-BLG-0026 using Keck and Subaru and compare it to the predictions of H2013 and stellar models. We revisit the modeling of OGLE-2012-BLG-0026, including more photometric data, update estimates of the source radius, and use the new flux constraints from Keck and Subaru to draw new conclusions about the physical parameters of the system.

2. DETECTING LIGHT FROM THE LENS STAR

In most cases it is possible to detect and to study (or to put upper limits on) the host lens stars with high angular resolution observations with adaptive optics such as Keck

[16] Sagan Fellow.

(Sumi et al. 2010; Batista et al. 2014, 2015), the Very Large Telescope (Donatowicz et al. 2008; Janczak et al. 2010; Batista et al. 2011; Kubas et al. 2012), Subaru (Fukui et al. 2015), GEMINI, MAGELLAN, and space-based observations with *Hubble Space Telescope* (Bennett et al. 2007; Dong et al. 2009; Bennett et al. 2015). High angular resolution allows us to resolve the source star from its unrelated neighbors, while the source and lens stars will generally still be blended together. Indeed, at the time of the microlensing event, the lens star must be less than ∼1 mas away from the source. The relative proper motion being typically ∼5 mas yr^{-1}, it will take several years to detect a centroid shift of the blended lens and source (Bennett et al. 2007) and more than a decade to finally see the lens and the source well-separated (Batista et al. 2015; Bennett et al. 2015).

Fortunately, it is possible to derive strong constraints shortly after the end of the microlensing event. Indeed, the microlensing models determine the *H*-band brightness of the source star, so it is usually possible to determine the H-band brightness of the host star (lens) by subtracting the source flux from the high angular resolution measurement of the combined host+source flux. This measurement can be used with a mass-distance relation, as in Equation (1) from Bennett et al. (2007), and an *H*-band mass–luminosity relation to yield a unique solution for the host star mass. This would yield a planetary mass and star–planet separation in physical units because the planet–star mass ratio and the separation in Einstein radius units are already known from the microlensing light curve.

2.1. Keck and Subaru Observations

The field containing the source star OGLE-2012-BLG-0026 has been observed by the VISTA 4 m telescope in JHK as part of the VVV survey (Minniti et al. 2010) monitoring the disk and the bulge of our galaxy. We developed a suite of tools using `astropy`[17] (Astropy Collaboration et al. 2013), `astroML` (Vanderplas et al. 2012), `TOPCAT` (Taylor 2005), and the `AstrOmatic` programs `SExtractor` (Bertin & Arnouts 1996) and `PSFEx` (Bertin 2011). We extracted JHK images centered on the target from the ESO archive and performed point-spread function (PSF) photometry. We performed astrometric and photometric calibrations using the 2MASS survey (Skrutskie et al. 2006). The resulting catalogs will be used to calibrate the AO data.

First, we used the Keck II telescope on Mauna Kea, with the NIRC2 imager and laser guide star, at medium resolution (pixel scale of 0.02 arcsec and a field of view of 20 arcsec). We obtained 5 H-band images with an exposure time of 30 s each on 2012 May 6 (HJD = 2456062.081), while the source star was still magnified by $A = 1.76$. The individual exposures were obtained in a dithered pattern with an amplitude of 1 arcsec. We observed a second epoch on 2012 July 28 (HJD = 2456134.834) with the IRCS camera on Subaru while the source was amplified by $A = 1.20$. We obtained 20 dithered exposures of 30 s each.

The Keck and Subaru observations were reduced with the same procedure described by Batista et al. (2014). For each data set, we first correct for the dark current and the flat-fielding using standard procedures. Using the catalogs we generated from VVV images we compute a first astrometric solution for each image. We then adopt one AO image as a reference, and build up a catalog of sources using `SExtractor`. We refined the astrometry of the other frames using this catalog. We visually inspect the individual images, then use `SWARP` (Bertin 2010) to stack them. Figure 1 shows *H*-band images from VVV, Keck, and Subaru. We identify no bright companion within the PSF of the lensing survey telescopes, suggesting that the blended light observed by OGLE is actually lined up to better than 0.1 arcsec with the source.

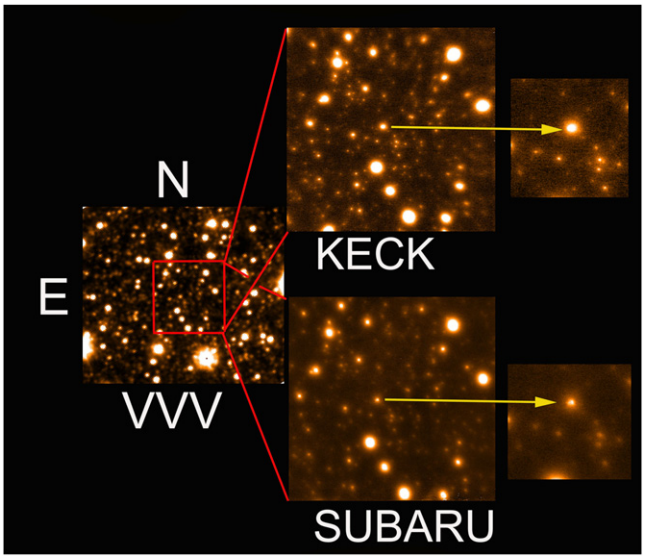

Figure 1. *H*-band images centered on the source of the microlensing event OGLE 2012-BLG-0026. The left insert is an *H*-band image obtained by the ESO VISTA 4 m telescope as part of the VVV survey. The upper right panel image was obtained with Keck, while the Subaru image is shown in the lower panel. They are both 18 arcsec square images. At the sub-arcsecond level, there are no bright stars close to the source contributing significantly to the observed blended light in OGLE photometry (4 arcsec images). Any bright blend would have to be aligned with the source to better than 0.1 arcsec.

We measured the flux of all sources in the field using `SExtractor` with aperture photometry. We cross-matched the VVV, Keck, and Subaru catalogs and determined the zero points. We then cross-identified Keck and Subaru sources to double check the consistency of the zero points. We obtained the following measurements of OGLE-2012-BLG-0026: $H_{\rm Keck} = 15.43 \pm 0.05$ while the source was amplified by 1.76, and $H_{\rm Subaru} = 15.60 \pm 0.05$ while the source was amplified by 1.20. The measured FWHMs are 130 mas for Keck and 170 mas for Subaru. There are no resolved blends contributing to the measured flux by the non-AO telescopes within ∼1 arcsec. The chance alignment of a blend with the source and lens to within the angular scale of the AO measurements is far lower than 1%, so we identify the origin of the blended light as the lens itself.

2.2. Estimating Extinction

H2013 estimated the extinction toward the source to be $A_I = 2.25$ by analyzing $(V - I,\ I)$ color–magnitude diagrams and using the constraint on the red clump position. This is compatible with the extinction maps provided by Gonzalez et al. (2012) that give $A_I = 2.27$ and $A_H = 0.525 \pm 0.09$ with the Nishiyama et al. (2009) extinction law. Following Bennett et al. (2015), we adopt $\tau_{\rm dust} = (0.120\ {\rm kpc})/\sin(b)$ (where b is the galactic latitude) as a scale height of the dust toward the galactic bulge. The extinction to the lens $A_{H_{\rm L}}$ as a function of

[17] http://www.astropy.org

the extinction to the source A_{H_S} and distances to the source D_S and to the lens D_L reads:

$$A_{H_L} = (1 - e^{-D_L/\tau_{dust}})/(1 - e^{-D_S/\tau_{dust}})A_{H_S}.$$

In the following, extinction to the lens will be estimated this way.

2.3. Constraining the Lens in the H-Band

An H-band light curve of the microlensing event was obtained by the ANDICAM camera mounted on the CTIO 1.3 m telescope. Using the model described in H2013 and performing the $(I - H)$ regression, we can compute the baseline flux of the source in the H-band to be $H_{S,fitted} = 16.56 \pm 0.01$. Using the Keck and Subaru measurements, we estimate the light coming from the lens to be $H_{L,Keck} = 16.48 \pm 0.13$ and $H_{L,Subaru} = 16.34 \pm 0.10$. The weighted average of these two measurements gives $H_L = 16.39 \pm 0.08$. The lens is brighter than the source by $16 \pm 8\%$, slightly bluer than the source in $(V - I)$ by $\Delta(V - I) = -0.07$ and much bluer than the source in $(I - H)$ by $\Delta(I - H) = -0.41 \pm 0.08$.

3. REVISITING THE MODELING OF THE MICROLENSING EVENT OGLE-2012-BLG-0026

3.1. A New Estimate of the Source Star Size

H2013 converted $(V - I)$ color to $(V - K)$ via the Bessel and Brett relations (Bessell & Brett 1988) and used the Kervella et al. (2004) $V - K$ relation to obtain a source angular radius of $1.55 \pm 0.13\,\mu$as. It is well-known that the optical-infrared color–angular size relations are more accurate than the ones using only optical colors (Kervella et al. 2004; Boyajian et al. 2013, 2014), and we expect that conversion from $(V - I)$ to $(V - K)$ colors includes this same uncertainty seen in the optical color–angular size relations. Directly using the Kervella et al. (2004) $V - H$ relation, we obtain $1.58 \pm 0.10\,\mu$as. Nevertheless, we decided to use the surface brightness relation from Boyajian et al. (2013, 2014) that links $(V - H, H)$ magnitudes to angular radius:

$$\log(2\,\theta_*\,(\mu\text{as})) = 0.536654 + 0.072703\,(V - H) - 0.2\,H.$$

This relation is slightly more accurate than Kervella et al. (2004), incorporating more data and excluding some unreliable measurements. Moreover, the fit of their relation is performed in a narrower range of spectral types, providing a better match to the source star. More details will be given by Sumi et al. (2015, submitted to ApJ). Our revised value for the angular radius is $\theta_* = 1.54 \pm 0.10\,\mu$as. It is fully consistent with H2013 estimates.

3.2. Modeling the Photometric Light Curve with or without the Adaptive Observations Constraints

We follow the modeling approach described by Bennett (2010) and Bennett et al. (2010) for the two-planet system OGLE-2006-BLG-109. First, we take the data set presented in H2013 without alteration. We then add the CTIO H-band photometric light curve and I-band data obtained using the 0.61 m B&C telescope in New Zealand. In contrast with H2013, we also release the constraint on the distance to the source D_S. Instead, we assume that the source is a Galactic Bulge star following the distance distribution from the galactic

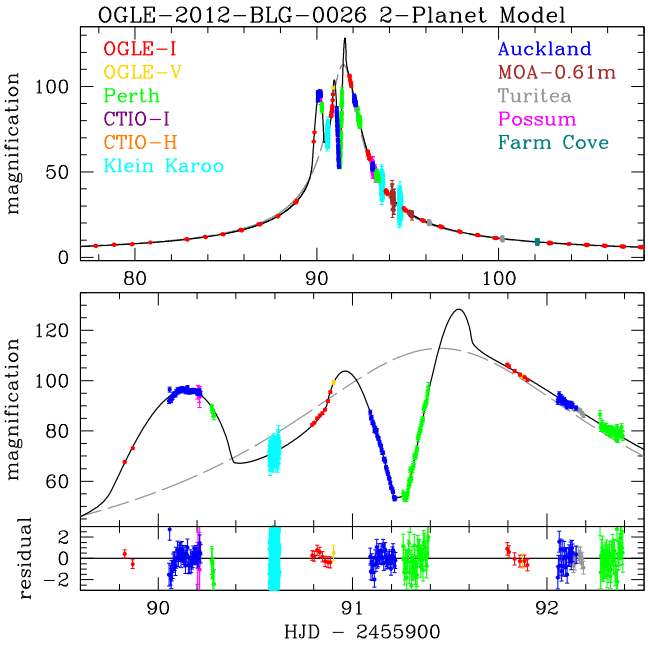

Figure 2. Top panel shows the complete photometric light curve and best-fit, two-planet model of OGLE-2012-BLG-0026. The different observatories are labeled and color-coded. The lower panel gives a zoom on the peak, the best model (solid line), and the point source point lens model (dashed line). The residuals of the best-fit model are plotted below. We used the same data sets as H2013, with the addition of CTIO 1.3 m H-band data, and I-band data from the MOA-0.61 m.

model used by Bennett et al. (2014). At this stage, we do not use the constraint from the measured light of the lens in the H-band in the modeling. There are eight degenerate solutions, with three two-fold degeneracies in the minimum impact parameter u_0 and the two-planet separations, and the χ^2 values for the 8 best-fit solutions in each local minima span a range of 10.2 in χ^2, from the best-fit $u_0 < 0$, $s_1 > 1$, $s_2 > 1$ solution to the least favored $u_0 > 0$, $s_1 > 1$, $s_2 < 1$ solution. The best-fit model has $\chi^2 = 3481.51$ for 3488 degrees of freedom. The overall geometries of the different models are very close to H2013, as shown in their Figure 2. To obtain a distribution of planetary system parameters that is consistent with the data, we run a series of Markov Chain Monte Carlos (MCMC) in each of the local minima with a weighing proportional to $e^{-\chi'^2}$. The final probability distribution is given by the weighted sum of the links in these chains.

The results of the MCMC runs are given as the first column in Table 1, labeled MOD0. We obtain a slightly larger Einstein ring radius $\theta_E = 0.96 \pm 0.05$ mas to be compared with value derived by H2013 of $\theta_E = 0.91 \pm 0.09$ mas and a slightly larger distance to the lens and to the source, with larger error bars. The parallax values of the models (A, C, D) from H2013 are slightly larger, and compatible within the error bars with the results reported here. For example, the model (C and D) from H2013 gives ($\pi_{E,N} = 0.001 \pm 0.028$, $\pi_{E,E} = 0.123 \pm 0.005$) and ($\pi_{E,N} = -0.07 \pm 0.05$, $\pi_{E,E} = 0.114 \pm 0.04$), to be compared with ($\pi_{E,N} = -0.004 \pm 0.03$, $\pi_{E,E} = 0.1089 \pm 0.04$) from our unconstrained fit MOD0.

In Figure 3, we show the mass and distance of the lens star derived by H2013 and our first model MOD0, which employs no lens brightness constraints. The MOD0 results were generated by a set MCMC over all eight of the degenerate solutions. The two results differ by more than one sigma, but

Table 1
Physical Parameters of the Two-planet System OGLE-2012-BLG-0026

Parameter	MOD0	MOD1	H2013 (D)
t_E (days)	94.00 ± 0.89	94.12 ± 0.92	···
D_L (kpc)	4.32 ± 0.43	4.019 ± 0.38	4.08 ± 0.30
D_s (kpc)	8.28 ± 1.44	7.39 ± 1.28	···
$x = D_L/D_S$	0.53 ± 0.047	0.55 ± 0.05	···
R_E (au)	4.12 ± 0.41	4.02 ± 0.38	···
θ_E (mas)	0.96 ± 0.048	0.98 ± 0.04	0.91 ± 0.09
M_* ($M_\odot$)	1.06 ± 0.05	1.06 ± 0.05	0.82 ± 0.13
M_{p1} (M_{Jup})	0.139 ± 0.0085	0.145 ± 0.0082	0.11 ± 0.02
M_{p2} (M_{Jup})	0.80 ± 0.07	0.86 ± 0.06	0.68 ± 0.10
D_{p1} (au)	3.94 ± 0.45	4.0 ± 0.5	3.82 ± 0.30
D_{p2} (au)	4.16 ± 0.45	4.8 ± 0.7	4.63 ± 0.37
$Mag_{lens}(H)$	16.69 ± 0.38	16.36 ± 0.13	···
$Mag_{lens}(I)$	19.23 ± 0.43	19.00 ± 0.23	···
$Mag_{lens}(V)$	21.75 ± 0.50	20.66 ± 0.15	···

Note. We show three different models. MOD0 is unconstrained by the luminosity of the lens. It shows the impact of the additional light curve data set and estimate for the source angular size, and can be directly compared to H2013 (from their Table 2). MOD1 is the best model, including constraints from the AO observations and Padova isochrones with uniform prior on disk star formation history. t_E is the Einstein ring crossing time, D_L and D_S are the distance to the lens and to the source, respectively. R_E is the Einstein ring radius in au, while θ_E is in milliarcseconds. The host star has a mass of M_*, while the two planets are of masses M_{p1} and M_{p2}, with semimajor axes of D_{p1} and D_{p2}, respectively. We also provide estimates for the V, I, H magnitudes of the lens host star.

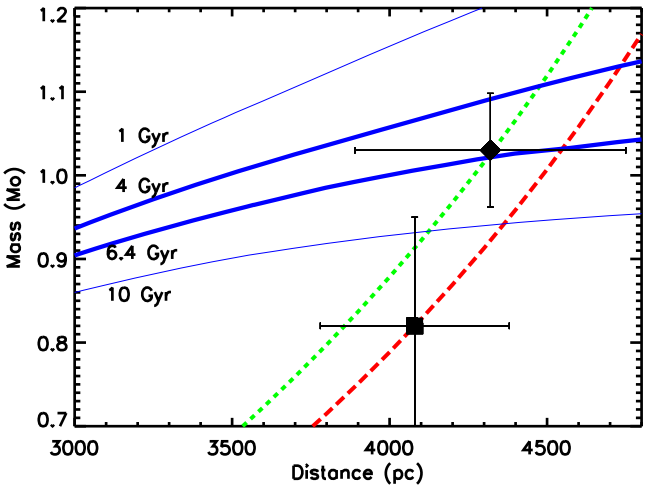

Figure 3. Mass–distance relations. The H2013 solution is shown as a square, while the diamond is the first model computed in Section 3.2. The long dashed red line shows the relation $M/M_\odot = \Theta_E^2(8\,\mathrm{kpc}/D_s)x/(1-x)$ for the parameters from H2013 and the dashed green line shows the parameters of our MOD0 model. The measured H-band magnitude for the lens is $H_L = 16.39 \pm 0.08$. We assume that the extinction to the lens is given by Equation (1), and we plot the mass-distance relation for the 1, 4, 6.4, 10 Gyr isochrones from Bertelli et al. (2008).

agree on the general features: the lens star is in the disk at ≈4 kpc, with a mass in the range ≈0.8–1.1 $M_\odot$. Comparison to the theoretical stellar isochrones computed by the Padova group (Bertelli et al. 2008) for solar metallicity and helium abundance $Y = 0.30$ shows good consistency with a typical main-sequence disk star of solar metallicity and an age of ∼6.4 Gyr. The 1σ error extends from 4 to ∼9 Gyr.

We now apply and rerun our MCMC runs with the addition of lens brightness constraints from the Keck and Subaru images. We consider two priors concerning the star formation history in the galactic disk: (1) a uniform star formation over 10 Gyr, and (2) an enhanced star formation over the 4–6 Gyr period. This prior on the star formation history has little impact on the result. The best-fit χ^2 for each model is typically raised by $\Delta\chi^2 \sim 0$–2. The exception is the previously most favored $u_0 < 0$, $s_1 > 1$, $s_2 > 1$ solution, which sees its χ^2 increased by $\Delta\chi^2 = 4.44$. The best fit is now the $u_0 > 0$, $s_1 > 1$, $s_2 > 1$ solution, which sees its χ^2 increase by $\Delta\chi^2 = 0.31$ to $\chi^2 = 3482.96$ for 3489 degrees of freedom. The worst fit for any of the local χ^2 minima is the $u_0 > 0$, $s_1 > 1$, $s_2 < 1$ solution, which has $\Delta\chi^2 = 8.78$ compared to the best-fit constrained solution. We report the results as MOD1 in Table 1. Finally, we take the original MOD0 modeling, and apply the posterior Keck/Subaru constraints and star formation constraints to this unconstrained model, i.e., to the MOD0 results from the MCMC run. The results are identical to MOD1. We note that the three modeling approaches yield the same central host mass, very similar values for the two planets, and small differences in distance to the source and to the lens. All the estimates are well within the reported 1σ error.

4. DISCUSSION AND CONCLUSION

We revisited the microlensing event OGLE-2012-BLG-0026. We confirm the physical picture of a two-planet system of gas giants orbiting a G star. We improved upon previous modeling and refined the parameters of the system by adding photometric light curves that were excluded by H2013. The adaptive optics observations provide further information by measuring the lens flux. The result is an increased estimate of the mass of the host star, to $M = 1.06 \pm 0.05\,M_\odot$. Using the H-band apparent magnitude of the lens, the reddening to the lens, and theoretical isochrones of stellar metallicity, we find good consistency for a stellar age of ≈4–6 Gyr. When using all the photometric data, this microlensing event is very well constrained. When we add the Keck and Subaru constraints to the modeling, or apply the constraints a posteriori, it confirms our initial model, but does not allow refinement of the physical parameters of the planets. The physical parameters are now known to ∼5%.

The central star is orbited by two cold giant planets of $0.145 \pm 0.008\,M_{Jup}$ and $0.86 \pm 0.07\,M_{Jup}$, at projected distances of 4.0 ± 0.5 au and 4.8 ± 0.7 au, respectively. Because the true orbital radii are equal to or larger than the projected separations, the planets are guaranteed to be well beyond the snow line for a G star. The inner planet of OGLE-2012-BLG-0026 is roughly half the mass of Saturn, while the outer one is closer to Jupiter. The two orbits are close. Compared to the original results, we find a more massive host star and more massive planets, orbiting at slightly larger projected distances.

An inspection of the mass histograms of hot and cold planets referenced in the Extrasolar Planets Encyclopædia[18] suggests that there is a dip at $\sim 45\,M_\oplus = 0.141\,M_{Jup}$. The lower-mass planet falls perfectly in the dip of the histogram. However, this mass histogram is obtained by combining results from different methods without accounting for their detection efficiencies and biases. In order to know if these two planets have any special properties, we decided to compare their masses with the mass distribution for quiet GK dwarf planet hosts detected by Kepler, and the microlensing mass function. We build the

[18] http://exoplanet.eu, referenced in 2015 October.

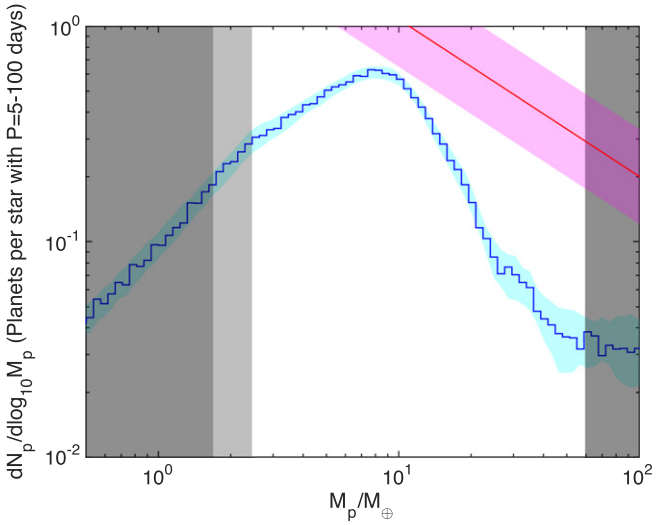

Figure 4. Mass histogram for planets orbiting GK dwarfs over periods in the range of 5–100 days discovered by *Kepler*. The upper left lines show the mass function for cold planets derived by Cassan et al. (2012).

Kepler-mass distribution for quiet GK dwarf planet hosts using the planet radius distribution from Petigura et al. (2013) and the Wolfgang et al. (2015) probabilistic mass–radius distribution based on the sample of transiting planets up to 8 $R_\oplus$ with radial velocity measurements. It is shown as Figure 4. The dark gray shaded regions indicate the edges of the mass–radius relation being used: specifically, below 1.7 $M_\oplus$ and above 60 $M_\oplus$ (where planets $\gtrsim$8 $R_\oplus$), which corresponds to the upper limit of the mass–radius sample on which the Wolfgang et al. mass–radius relation was based. The pale gray region denotes the regime where incompleteness due to the small radius cutoff at 1 $R_\oplus$ in the Petigura et al. radius function could start to be significant. The cyan shaded region accounts for the error bars quoted on the Petigura et al. radius distribution, containing 68% of the mass-distributions obtained when we sampled from (Gaussian-approximated) uncertainties on the planet occurrence in each radius bin. The *y*-axis of the figure is normalized such that the area under the curve gives the number of planets per star (on orbits 5–100 days) within the $\log(M_p)$ range chosen. We remark that the planet mass distribution maybe dominated by the uncertainty in the mass–radius distribution, which is not reflected in the error range plotted. We then overplot the mass function from Cassan et al. (2012) $dN/(d\log(a)d\log(M) = 10^{-0.62\pm0.22}(M/M_{\rm sat})^{-0.73\pm0.17}$ (where $M_{\rm sat} = 95\,M_\oplus$). First, we recall that the microlensing mass function is restricted to planets beyond the snow line over orbits in the range 0.5–10 au, and spanning from 5 $M_\oplus$ to $M_{\rm Jup}$. We have a larger abundance of cold planets, which is not surprising since it focuses on planets that most likely have not migrated far from their location of formation. Second, the steep slope of the microlensing mass function comes from the statistics of Cassan et al. (2012) combining into a single power law the two populations of gaseous giants, and super-Earth/Mini-Neptune. The results from *Kepler* would suggest that it is probably better to separate gaseous giant, from Super-Earth/Mini Neptunes, which will be possible with the impeding increase of microlensing detections thanks to the new ground-based facilities such as the global worldwide network of wide-field imagers (OGLE, MOA, *WISE*, UTGO, KMTNet), the *K2* microlensing campaign, Euclid, and WFIRST.

Figure 4 is therefore very different from the uncorrected mass distribution extracted from the Extrasolar Planets Encyclopædia. The ∼45 $M_\oplus$ dip in the mass histogram is only due to selection effects. The lower-mass planet in the OGLE-2012-BLG-0026 system is a gaseous giant with no special properties.

The masses of the two cold gaseous planets orbiting the solar-like star OGLE-2012-BLG-0026 are constrained to 5%. We also have derived a constraint on its age, corresponding to the standard age of disk stars for a solar metallicity. The projected separations of the two planets appear similar, at 4.0 ± 0.5 and 4.8 ± 0.7 au. However, this is only the instantaneous, projected separation of the two planets; their true orbital semimajor axes and eccentricities remain unknown. In addition there is also the well-known close–wide degeneracy in the microlensing solution for each planet. Therefore we cannot definitively describe the orbital architecture of the system; the planets could be co-orbital, or could be separated by tens of au. Smith & Lissauer (2009) find that two prograde-orbiting planets separated by several mutual Hill radii ($r_{\rm H}$) are indefinitely stable; for the masses in Table 1, under the rather unlikely assumption that the semimajor axes are equal to the projected separations, $r_{\rm H} \approx 0.3$ au. Thus the raw numbers for the best-fit system parameters could suggest instability. Barnes & Greenberg (2007) find that many multi-planet systems lie very close to instability, as predicted by the Hill criterion, but are stabilized by mean motion resonances; additionally they make the claim that multi-planet systems tend to be packed, such that additional planets on formally stable orbits could not be fit in between the detected planets. This principle could guide future work in attempting to further characterize the geometry of multi-planet microlensing systems. Given the degeneracies in the OGLE-2012-BLG-0026b and OGLE-2012-BLG-0026c orbits, we cannot draw any further conclusions about the stability of the system. Unless the system is quite close to being face-on, the orbits and the orbital separations are likely to be significantly larger than shown in Table 1; for any separations larger than ∼1 au the system is expected to be indefinitely stable.

Given the absence of blends at the arcsecond scale and the fact that the lens is brighter than the source, it will be possible in the future to directly measure the metallicity with spectroscopy using 8 m class telescopes.

V.B. was supported by the CNES and the DIM ACAV, Région Île-de-France. V.B., J.P.B., and J.B.M. acknowledge the support of PERSU Sorbonne Université the Programme National de Planétologie and the labex ESEP. We are grateful to F. Naudin for discussions about the properties of this system. D.P.B. was supported by grants NASA-NNX12AF54G, JPL-RSA 1453175, and NSF AST-1211875. F.A. is supported by JSPS23340064. Work by C.H. was supported by the Creative Research Initiative Program (2009-0081561) of the National Research Foundation of Korea. J.P.B. thanks the University of Tasmania for support as part of their visiting scholar program. We thank David and Michelle Warren for their support. This work was partially supported by a NASA Keck PI Data Award, administered by the NASA Exoplanet Science Institute. The data presented herein were obtained at the WM Keck Observatory from telescope time allocated to the National

Aeronautics and Space Administration through the agency scientific partnership with the California Institute of Technology and the University of California. The Observatory was made possible by the generous financial support of the WM Keck Foundation. Work by J.C.Y. and L.A.R. was performed under contract with the California Institute of Technology (Caltech)/Jet Propulsion Laboratory (JPL), funded by NASA through the Sagan Fellowship Program executed by the NASA Exoplanet Science Institute. This research made use of `astropy`, a community-developed core Python package for Astronomy, `astroML`, and `TOPCAT`. This publication makes use of data products from the Two Micron All Sky Survey, which is a joint project of the University of Massachusetts and the Infrared Processing and Analysis Center/California Institute of Technology, funded by the National Aeronautics and Space Administration and the National Science Foundation. This work is based on data products from observations made with ESO Telescopes at the La Silla or Paranal Observatories under ESO programme ID 179.B-2002.

REFERENCES

Astropy Collaboration, Robitaille, T. P., Tollerud, E. J., et al. 2013, A&A, 558, A33
Barnes, R., & Greenberg, R. 2007, ApJL, 665, L67
Batista, V., Beaulieu, J.-P., Bennett, D. P., et al. 2015, ApJ, 808, 170
Batista, V., Beaulieu, J.-P., Gould, A., et al. 2014, ApJ, 780, 54
Batista, V., Gould, A., Dieters, S., et al. 2011, A&A, 529, A102
Bennett, D. P. 2010, ApJ, 716, 1408
Bennett, D. P., Anderson, J., & Gaudi, B. S. 2007, ApJ, 660, 781
Bennett, D. P., Batista, V., Bond, I. A., et al. 2014, ApJ, 785, 155
Bennett, D. P., Bhattacharya, A., Anderson, J., et al. 2015, ApJ, 808, 169
Bennett, D. P., Rhie, S. H., Nikolaev, S., et al. 2010, ApJ, 713, 837
Bertelli, G., Girardi, L., Marigo, P., & Nasi, E. 2008, A&A, 484, 815
Bertin, E. 2010, Astrophysics Source Code Library, ascl:1010.068
Bertin, E. 2011, in ASP Conf. Ser. 442, Astronomical Data Analysis Software and Systems XX, ed. I. N. Evans et al. (San Francisco, CA: ASP), 435
Bertin, E., & Arnouts, S. 1996, A&AS, 117, 393
Bessell, M. S., & Brett, J. M. 1988, PASP, 100, 1134
Boyajian, T. S., von Braun, K., van Belle, G., et al. 2013, ApJ, 771, 40
Boyajian, T. S., von Braun, K., van Belle, G., et al. 2014, ApJ, 787, 92
Cassan, A., Kubas, D., Beaulieu, J.-P., et al. 2012, Natur, 481, 167
Donatowicz, J., Beaulieu, J. P., Batista, V., et al. 2008, in ASP Conf. Ser. 398, Extreme Solar Systems, ed. D. Fischer et al. (San Francisco, CA: ASP), 499
Dong, S., Gould, A., Udalski, A., et al. 2009, ApJ, 695, 970
Fukui, A., Gould, A., Sumi, T., et al. 2015, ApJ, 809, 74
Gaudi, B. S., Bennett, D. P., Udalski, A., et al. 2008, Sci, 319, 927
Gonzalez, O. A., Rejkuba, M., Zoccali, M., et al. 2012, A&A, 543, A13
Han, C., Udalski, A., Choi, J.-Y., et al. 2013, ApJL, 762, L28
Janczak, J., Fukui, A., Dong, S., et al. 2010, ApJ, 711, 731
Kervella, P., Bersier, D., Mourard, D., et al. 2004, A&A, 428, 587
Kubas, D., Beaulieu, J. P., Bennett, D. P., et al. 2012, A&A, 540, A78
Minniti, D., Lucas, P. W., Emerson, J. P., et al. 2010, NewA, 15, 433
Nishiyama, S., Tamura, M., Hatano, H., et al. 2009, ApJ, 696, 1407
Petigura, E. A., Marcy, G. W., & Howard, A. W. 2013, ApJ, 770, 69
Skrutskie, M. F., Cutri, R. M., Stiening, R., et al. 2006, AJ, 131, 1163
Smith, A. W., & Lissauer, J. J. 2009, Icar, 201, 381
Sumi, T., Bennett, D. P., Bond, I. A., et al. 2010, ApJ, 710, 1641
Taylor, M. B. 2005, in ASP Conf. Ser. 347, Astronomical Data Analysis Software and Systems XIV, ed. P. Shopbell, M. Britton, & R. Ebert (San Francisco, CA: ASP), 29
Vanderplas, J., Connolly, A., Ivezić, Ž, & Gray, A. 2012, in Proc. of Conf. on Intelligent Data Understanding (CIDU), (IEEE), 47
Wolfgang, A., Rogers, L. A., & Ford, E. B. 2015, arXiv:1504.07557